

# ANALYSIS OF 3D RIGID BODY MOTION USING THE NINE ACCELEROMETER ARRAY AND THE RANDOMLY DISTRIBUTED IN-PLANE ACCELEROMETER SYSTEMS

**Erik G. Takhounts**

NHTSA

**Vikas Hasija**

GESAC, Inc

**Rolf H. Eppinger**

NHTSA (retired)

United States

Paper Number: 09-0402

## ABSTRACT

The nine accelerometer array sensor package is used extensively in injury biomechanics research to obtain the rotational acceleration time histories of a rigid body. It has been shown in the past to remain computationally stable while the alternative, the six accelerometer array, becomes unstable in the presence of small inaccuracies in the individually measured accelerations. The nine accelerometer array process achieves its stability by requiring the measurement of three rotational accelerations, thus eliminating the six accelerometer array's dependency on having knowledge of the rigid body's three rotational velocities at each instant in time. The nine accelerometer array's additional three measurements also provide other important benefits: 1. Identifying whether or not any one of the nine translational acceleration measurements is inconsistent with rigid body motion, 2. If an incorrect acceleration is found, determining what the actual time history should be for that case, 3. Use of optimization methodology to obtain the best possible solution for the rigid body motion. This paper presents the derivation of an additional set of constraint equations that a given set of nine linear accelerations must satisfy to be consistent with rigid body motion, demonstrates how an inconsistent acceleration input is discovered, and describes the process by which the true time history of the acceleration is recovered. In addition, optimization methodology is introduced to obtain the best possible solution for a randomly distributed in-plane accelerometer system when errors in measurements are artificially introduced.

## INTRODUCTION

The Nine Accelerometer Array Package (NAAP) uses translational accelerations to describe the angular motion of a rigid body. It has been used extensively in injury biomechanics research to obtain human and dummy head 3D kinematics (Hardy et al., 2001, 2007, Takhounts et al., 2003, 2008). This sensor package typically uses nine accelerometers

placed in a 3-2-2 configuration (Figure 1) to track the motion of a rigid body (Padgaonkar et al., 1975). The advantage of this configuration was shown to be in the stability of the NAAP when compared to the six accelerometer array (Figure 2) which required the knowledge of rotational velocities at each instant of time. This stability advantage of the NAAP is achieved at the expense of measuring three additional translational accelerations (in Figure 1 the three additional accelerations are  $a_{2x}$ ,  $a_{3x}$ , and  $a_{3y}$ ).

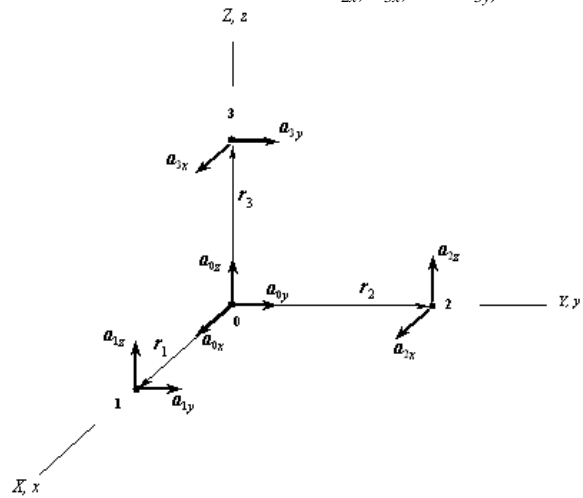


**Figure 1. Nine accelerometer array configuration.**

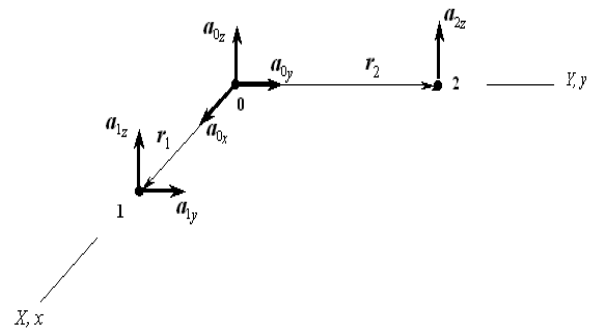


**Figure 2. Six accelerometer array configuration.**

It will be shown in this paper that these three additional measurements are not independent and are subject to the rigid body constraints. To do so, first consider a general 3D motion of a rigid body (Figure 3) about a fixed point that is the same as the motion of point  $B$  measured by the observer located at point  $A$ .

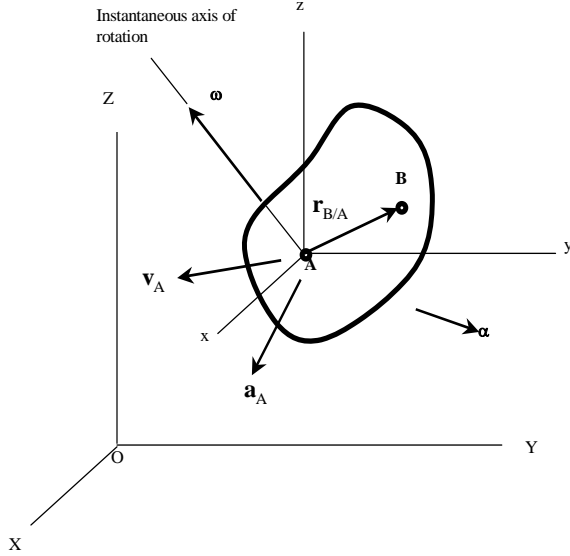


**Figure 3. Rigid body subjected to a 3D general motion.**

This relative motion occurs about the instantaneous center of rotation and is defined by:

$$\mathbf{v}_{B/A} = \boldsymbol{\omega} \times \mathbf{r}_{B/A} \quad (1)$$

$$\text{and} \quad \mathbf{a}_{B/A} = \boldsymbol{\alpha} \times \mathbf{r}_{B/A} + \boldsymbol{\omega} \times (\boldsymbol{\omega} \times \mathbf{r}_{B/A}), \quad (2)$$

where  $\mathbf{v}_{B/A}$  and  $\mathbf{a}_{B/A}$  are the relative velocity and acceleration of point  $B$  with respect to point  $A$ ,  $\boldsymbol{\omega}$  and  $\boldsymbol{\alpha}$  are rotational velocity and acceleration. For translating axes, the relative motions are related to absolute motions by  $\mathbf{v}_B = \mathbf{v}_A + \mathbf{v}_{B/A}$  and  $\mathbf{a}_B = \mathbf{a}_A + \mathbf{a}_{B/A}$ , and the absolute velocity and acceleration of point  $B$  are determined from the following equations:

$$\mathbf{v}_B = \mathbf{v}_A + \boldsymbol{\omega} \times \mathbf{r}_{B/A} \quad (3)$$

$$\mathbf{a}_B = \mathbf{a}_A + \boldsymbol{\alpha} \times \mathbf{r}_{B/A} + \boldsymbol{\omega} \times (\boldsymbol{\omega} \times \mathbf{r}_{B/A}). \quad (4)$$

If the vectors are defined as:  $\mathbf{a}_A = [a_{Ax}, a_{Ay}, a_{Az}]^T$ ,  $\mathbf{a}_B = [a_{Bx}, a_{By}, a_{Bz}]^T$ ,  $\boldsymbol{\alpha} = [\alpha_x, \alpha_y, \alpha_z]^T$ ,  $\boldsymbol{\omega} = [\omega_x, \omega_y, \omega_z]^T$ , and  $\mathbf{r}_{B/A} = [r_x, r_y, r_z]^T$ , then equation 4 can be rewritten in the component form:

$$\begin{bmatrix} a_{Bx} \\ a_{By} \\ a_{Bz} \end{bmatrix} = \begin{bmatrix} a_{Ax} \\ a_{Ay} \\ a_{Az} \end{bmatrix} + \begin{bmatrix} \alpha_y r_z - \alpha_z r_y \\ \alpha_z r_x - \alpha_x r_z \\ \alpha_x r_y - \alpha_y r_x \end{bmatrix} + \begin{bmatrix} \omega_x (\omega_y r_y + \omega_z r_z) - r_x (\omega_y^2 + \omega_z^2) \\ \omega_y (\omega_z r_z + \omega_x r_x) - r_y (\omega_z^2 + \omega_x^2) \\ \omega_z (\omega_x r_x + \omega_y r_y) - r_z (\omega_x^2 + \omega_y^2) \end{bmatrix} \quad (5)$$

Equations 5 will be used extensively throughout the paper in deriving both – the closed form constraints equations for the NAAP and the optimization based solution for a randomly distributed in-plane accelerometer system.

## METHODOLOGY

### NAAP Constraints Equations

Consider the 3-2-2-2 NAAP configuration illustrated in Figure 1 arranged within a rigid body. The accelerations of points 1, 2, and 3 with respect to point 0 can be expressed using equations 5. For points 1 and 0 substitute 1 for  $B$ , 0 for  $A$ ,  $\mathbf{r}_{B/A} = \mathbf{r}_1 = [r_x, 0, 0]^T$ , where  $r_x$  is the distance between points 1 and 0:

$$\begin{bmatrix} - \\ a_{1y} \\ a_{1z} \end{bmatrix} = \begin{bmatrix} - \\ a_{0y} \\ a_{0z} \end{bmatrix} + \begin{bmatrix} - \\ \alpha_z r_x \\ -\alpha_y r_x \end{bmatrix} + \begin{bmatrix} - \\ \omega_y \omega_x r_x \\ \omega_z \omega_x r_x \end{bmatrix}. \quad (6)$$

Similarly, for points 2 and 0, substitute 2 for  $B$ , 0 for  $A$ ,  $\mathbf{r}_{B/A} = \mathbf{r}_2 = [0, r_y, 0]^T$ , where  $r_y$  is the distance between points 2 and 0:

$$\begin{bmatrix} a_{2x} \\ - \\ a_{2z} \end{bmatrix} = \begin{bmatrix} a_{0x} \\ - \\ a_{0z} \end{bmatrix} + \begin{bmatrix} -\alpha_z r_y \\ - \\ \alpha_x r_y \end{bmatrix} + \begin{bmatrix} \omega_x \omega_y r_y \\ - \\ \omega_z \omega_y r_y \end{bmatrix}. \quad (7)$$

For points 3 and 0, substitute 3 for  $B$ , 0 for  $A$ ,  $\mathbf{r}_{B/A} = \mathbf{r}_3 = [0, 0, r_z]^T$ , where  $r_z$  is the distance between points 3 and 0:

$$\begin{bmatrix} a_{3x} \\ a_{3y} \\ - \end{bmatrix} = \begin{bmatrix} a_{0x} \\ a_{0y} \\ - \end{bmatrix} + \begin{bmatrix} \alpha_y r_z \\ -\alpha_x r_z \\ - \end{bmatrix} + \begin{bmatrix} \omega_x \omega_z r_z \\ \omega_y \omega_z r_z \\ - \end{bmatrix}. \quad (8)$$

From equations 7 and 8,  $\alpha_x$  is found to be:

$$\begin{cases} \alpha_x = \frac{a_{2z} - a_{0z}}{r_y} - \omega_y \omega_z \\ \alpha_x = -\frac{a_{3y} - a_{0y}}{r_z} + \omega_y \omega_z \end{cases} \quad (9)$$

Similarly,  $\alpha_y$  is found from equations 6 and 8:

$$\begin{cases} \alpha_y = -\frac{a_{1z} - a_{0z}}{r_x} + \omega_z \omega_x \\ \alpha_y = \frac{a_{3x} - a_{0x}}{r_z} - \omega_z \omega_x \end{cases} \quad (10)$$

and  $\alpha_z$  is found from equations 6 and 7:

$$\begin{cases} \alpha_z = \frac{a_{1y} - a_{0y}}{r_x} - \omega_x \omega_y \\ \alpha_z = -\frac{a_{2x} - a_{0x}}{r_y} + \omega_x \omega_y \end{cases} \quad (11)$$

By adding the paired equations 9, 10, and 11, the three angular accelerations  $\alpha_x$ ,  $\alpha_y$ , and  $\alpha_z$  can be expressed as functions of the nine translational accelerations and the arm lengths, i.e.:

$$\begin{cases} \alpha_x = \frac{a_{2z} - a_{0z}}{2r_y} - \frac{a_{3y} - a_{0y}}{2r_z} \\ \alpha_y = \frac{a_{3x} - a_{0x}}{2r_z} - \frac{a_{1z} - a_{0z}}{2r_x} \\ \alpha_z = \frac{a_{1y} - a_{0y}}{2r_x} - \frac{a_{2x} - a_{0x}}{2r_y} \end{cases} \quad (12)$$

Equations 12 are given in Padgaonkar et al. (1975), and currently serve as the basis for derivation of angular motion of a rigid body from a set of nine translational accelerations. Translational accelerations, as shown in equations 12, are usually functions of time. Therefore, angular velocities of the rigid body could be obtained by simply integrating equations 12 with respect to time:

$$\begin{cases} \omega_x(t) = \int \alpha_x(t) dt \\ \omega_y(t) = \int \alpha_y(t) dt \\ \omega_z(t) = \int \alpha_z(t) dt \end{cases} \quad (13)$$

However, by subtracting the paired equations 9, 10, and 11 from each other, another set of equations can be found:

$$\begin{cases} \omega_y \omega_z = \frac{a_{2z} - a_{0z}}{2r_y} + \frac{a_{3y} - a_{0y}}{2r_z} \\ \omega_z \omega_x = \frac{a_{3x} - a_{0x}}{2r_z} + \frac{a_{1z} - a_{0z}}{2r_x} \\ \omega_x \omega_y = \frac{a_{1y} - a_{0y}}{2r_x} + \frac{a_{2x} - a_{0x}}{2r_y} \end{cases} \quad (14)$$

To fully describe a general 3D motion of a rigid body in space and time all nine equations 12 – 14 must be satisfied. This implies that nine measured acceleration in a NAAP configuration are not independent functions of time, but rather are bound by the additional set of equations (14). Let's call these equations – rigid body constraint equations.

To illustrate this point, consider a simple example of pure rotation of a rigid body where:

$$a_{0x}(t) = a_{0y}(t) = a_{0z}(t) = 0, \quad (15)$$

and the remaining six accelerations are identical functions of time:

$$a_{1y}(t) = a_{1z}(t) = a_{2x}(t) = a_{2z}(t) = a_{3x}(t) = a_{3y}(t) = t. \quad (16)$$

Then, equations (12) become:

$$\begin{cases} \alpha_x(t) = \frac{t}{2r_y} - \frac{t}{2r_z} \\ \alpha_y(t) = \frac{t}{2r_z} - \frac{t}{2r_x} \\ \alpha_z(t) = \frac{t}{2r_x} - \frac{t}{2r_y} \end{cases} \quad (17)$$

Integrating these equations (17) with respect to time gives the following angular velocities:

$$\begin{cases} \omega_x(t) = \frac{t^2}{4r_y} - \frac{t^2}{4r_z} \\ \omega_y(t) = \frac{t^2}{4r_z} - \frac{t^2}{4r_x} \\ \omega_z(t) = \frac{t^2}{4r_x} - \frac{t^2}{4r_y} \end{cases} \quad (18)$$

Using equations 18, the products of the angular velocities are found to be:

$$\begin{cases} \omega_y(t)\omega_z(t) = -\frac{t^4(r_x - r_y)(r_x - r_z)}{16r_x^2 r_y r_z} \\ \omega_z(t)\omega_x(t) = \frac{t^4(r_x - r_y)(r_y - r_z)}{16r_x r_y^2 r_z} \\ \omega_x(t)\omega_y(t) = -\frac{t^4(r_x - r_z)(r_y - r_z)}{16r_x r_y r_z^2} \end{cases} \quad (19)$$

However, substituting equations 15 and 16 into 14 directly yields another relationship for the products of the angular velocities:

$$\begin{cases} \omega_y(t)\omega_z(t) = \frac{t}{2r_y} + \frac{t}{2r_z} \\ \omega_z(t)\omega_x(t) = \frac{t}{2r_z} + \frac{t}{2r_x} \\ \omega_x(t)\omega_y(t) = \frac{t}{2r_x} + \frac{t}{2r_y} \end{cases} \quad (20)$$

Comparing equations 19 and 20 and noticing their inequality it can be concluded that the conditions 12, 13, and 14 cannot be satisfied simultaneously if nine translational accelerations are chosen in the arbitrary form of 15 and 16. In other words, in order to satisfy equations 12, 13, and 14, the nine translational accelerations cannot be arbitrary functions of time.

### Closed Form Solutions for an Erroneous Channel in NAAP

Suppose it is known that one of the accelerations in Figure 1, e.g.  $a_{1y}(t)$ ,  $a_{1z}(t)$ ,  $a_{2x}(t)$ ,  $a_{2z}(t)$ ,  $a_{3x}(t)$ , or  $a_{3y}(t)$  is not measured properly or missing. Assume first for the sake of simplicity that the accelerations at point 0  $a_{0x}(t)$ ,  $a_{0y}(t)$ , and  $a_{0z}(t)$  are measured properly. To identify and correct the improperly measured trace

equations 12 – 14 will be used. From the first set of equations (14) the acceleration trace  $a_{2z}(t)$  can be expressed as:

$$a_{2z}(t) = 2r_y \left( \omega_y(t) \omega_z(t) - \frac{a_{3y}(t) - a_{0y}(t)}{2r_z} \right) + a_{0z}(t). \quad (21)$$

Using equations 13 for  $\omega_y(t)$  and  $\omega_z(t)$  and equations 12 for  $\alpha_y(t)$  and  $\alpha_z(t)$ , and substituting them into the equation above for  $a_{2z}(t)$  (21), we get:

$$\begin{aligned} a_{2z}(t) &= 2r_y \left\{ \int_t \alpha_y(t) dt \int_t \alpha_z(t) dt - \frac{a_{3y}(t) - a_{0y}(t)}{2r_z} \right\} + a_{0z}(t) \\ &= 2r_y \left\{ \int_t \left[ \frac{a_{3x}(t) - a_{0x}(t)}{2r_z} - \frac{a_{1z}(t) - a_{0z}(t)}{2r_x} \right] dt \int_t \left[ \frac{a_{1y}(t) - a_{0y}(t)}{2r_x} - \frac{a_{2x}(t) - a_{0x}(t)}{2r_y} \right] dt \right. \\ &\quad \left. - \frac{a_{3y}(t) - a_{0y}(t)}{2r_z} \right\} + a_{0z}(t) \end{aligned} \quad (22)$$

In a functional form the above equation can be rewritten:

$$a_{2z}(t) = f[a_{0x}(t), a_{0y}(t), a_{0z}(t), a_{1x}(t), a_{1y}(t), a_{1z}(t), a_{2x}(t), a_{2y}(t), a_{2z}(t), r_x, r_y, r_z] \quad (22a)$$

It should be observed that the acceleration trace  $a_{2z}(t)$  is a function of all the other eight acceleration traces in the array and the distances  $r_x$ ,  $r_y$ , and  $r_z$ . This means that if acceleration trace  $a_{2z}(t)$  was measured incorrectly, but all the rest traces were correct, the correct  $a_{2z}(t)$  can be calculated using equation 22. Similarly, for the rest accelerations the relationship will be:

$$\begin{aligned} a_{1y}(t) &= 2r_x \left\{ \int_t \alpha_x(t) dt \int_t \alpha_y(t) dt - \frac{a_{2x}(t) - a_{0x}(t)}{2r_y} \right\} + a_{0y}(t) \\ &= 2r_x \left\{ \int_t \left[ \frac{a_{2z}(t) - a_{0z}(t)}{2r_y} - \frac{a_{1z}(t) - a_{0z}(t)}{2r_z} \right] dt \int_t \left[ \frac{a_{3x}(t) - a_{0x}(t)}{2r_z} - \frac{a_{1x}(t) - a_{0x}(t)}{2r_x} \right] dt \right. \\ &\quad \left. - \frac{a_{2x}(t) - a_{0x}(t)}{2r_y} \right\} + a_{0y}(t) \end{aligned} \quad (23)$$

$$\begin{aligned} a_{1z}(t) &= 2r_x \left\{ \int_t \alpha_x(t) dt \int_t \alpha_z(t) dt - \frac{a_{3x}(t) - a_{0x}(t)}{2r_z} \right\} + a_{0z}(t) \\ &= 2r_x \left\{ \int_t \left[ \frac{a_{1y}(t) - a_{0y}(t)}{2r_x} - \frac{a_{2x}(t) - a_{0x}(t)}{2r_y} \right] dt \int_t \left[ \frac{a_{2z}(t) - a_{0z}(t)}{2r_y} - \frac{a_{3y}(t) - a_{0y}(t)}{2r_z} \right] dt \right. \\ &\quad \left. - \frac{a_{3x}(t) - a_{0x}(t)}{2r_z} \right\} + a_{0z}(t) \end{aligned} \quad (24)$$

$$\begin{aligned} a_{2x}(t) &= 2r_y \left\{ \int_t \alpha_x(t) dt \int_t \alpha_y(t) dt - \frac{a_{1y}(t) - a_{0y}(t)}{2r_z} \right\} + a_{0x}(t) \\ &= 2r_y \left\{ \int_t \left[ \frac{a_{2z}(t) - a_{0z}(t)}{2r_y} - \frac{a_{3y}(t) - a_{0y}(t)}{2r_z} \right] dt \int_t \left[ \frac{a_{3x}(t) - a_{0x}(t)}{2r_z} - \frac{a_{1x}(t) - a_{0x}(t)}{2r_x} \right] dt \right. \\ &\quad \left. - \frac{a_{1y}(t) - a_{0y}(t)}{2r_z} \right\} + a_{0x}(t) \end{aligned} \quad (25)$$

$$\begin{aligned} a_{3x}(t) &= 2r_z \left\{ \int_t \alpha_x(t) dt \int_t \alpha_z(t) dt - \frac{a_{1z}(t) - a_{0z}(t)}{2r_x} \right\} + a_{0x}(t) \\ &= 2r_z \left\{ \int_t \left[ \frac{a_{1y}(t) - a_{0y}(t)}{2r_x} - \frac{a_{2x}(t) - a_{0x}(t)}{2r_y} \right] dt \int_t \left[ \frac{a_{2z}(t) - a_{0z}(t)}{2r_y} - \frac{a_{3y}(t) - a_{0y}(t)}{2r_z} \right] dt \right. \\ &\quad \left. - \frac{a_{1z}(t) - a_{0z}(t)}{2r_x} \right\} + a_{0x}(t) \end{aligned} \quad (26)$$

$$\begin{aligned} a_{3y}(t) &= 2r_z \left\{ \int_t \alpha_y(t) dt \int_t \alpha_z(t) dt - \frac{a_{2z}(t) - a_{0z}(t)}{2r_x} \right\} + a_{0y}(t) \\ &= 2r_z \left\{ \int_t \left[ \frac{a_{3x}(t) - a_{0x}(t)}{2r_z} - \frac{a_{1z}(t) - a_{0z}(t)}{2r_x} \right] dt \int_t \left[ \frac{a_{1y}(t) - a_{0y}(t)}{2r_x} - \frac{a_{2x}(t) - a_{0x}(t)}{2r_y} \right] dt \right. \\ &\quad \left. - \frac{a_{2z}(t) - a_{0z}(t)}{2r_x} \right\} + a_{0y}(t) \end{aligned} \quad (27)$$

Each one of the six computed acceleration traces (22 through 27) in the nine accelerometer array can be compared with the corresponding originally measured acceleration trace. If one of the computed traces is not coincident with that originally measured, then the originally measured acceleration trace contains an error, and it should be replaced with the computed one. If more than one of the computed traces is not coincident with the corresponding originally measured traces, then the error could be in one of the three accelerations  $[a_{0x}(t), a_{0y}(t), \text{ or } a_{0z}(t)]$ , or may be due to more than one of the acceleration traces (or arm lengths) being measured improperly. To check for an incorrect trace, first let's derive additional equations for the three acceleration traces at point 0:  $a_{0x}(t)$ ,  $a_{0y}(t)$ , and  $a_{0z}(t)$ . From the second equation of set 14 and by using relations 12 and 13,  $a_{0x}(t)$  can be expressed as:

$$\begin{aligned} a_{0x}(t) &= -2r_z \left\{ \int_t \alpha_x(t) dt \int_t \alpha_z(t) dt - \frac{a_{1z}(t) - a_{0z}(t)}{2r_x} \right\} + a_{3x}(t) \\ &= -2r_z \left\{ \int_t \left[ \frac{a_{1y}(t) - a_{0y}(t)}{2r_x} - \frac{a_{2x}(t) - a_{0x}(t)}{2r_y} \right] dt \int_t \left[ \frac{a_{2z}(t) - a_{0z}(t)}{2r_y} - \frac{a_{3y}(t) - a_{0y}(t)}{2r_z} \right] dt \right. \\ &\quad \left. - \frac{a_{1z}(t) - a_{0z}(t)}{2r_x} \right\} + a_{3x}(t) \end{aligned} \quad (28a)$$

Similarly, from the third equation of set 14:

$$\begin{aligned} a_{0y}(t) &= -2r_x \left\{ \int_t \alpha_x(t) dt \int_t \alpha_y(t) dt - \frac{a_{1y}(t) - a_{0y}(t)}{2r_x} \right\} + a_{2x}(t) \\ &= -2r_x \left\{ \int_t \left[ \frac{a_{2z}(t) - a_{0z}(t)}{2r_y} - \frac{a_{3y}(t) - a_{0y}(t)}{2r_z} \right] dt \int_t \left[ \frac{a_{3x}(t) - a_{0x}(t)}{2r_z} - \frac{a_{1x}(t) - a_{0x}(t)}{2r_x} \right] dt \right. \\ &\quad \left. - \frac{a_{1y}(t) - a_{0y}(t)}{2r_x} \right\} + a_{2x}(t) \end{aligned} \quad (28b)$$

If equations 28a and 28b yield the same result, then all nine traces are self-consistent and no further investigation is required. However, if these equations

don't yield the same result, then the acceleration trace  $a_{0x}(t)$  should be expressed as a function of the remaining eight acceleration traces. One of the possible ways to accomplish this is to subtract equation 28b from 28a and solve the newly obtained equation for the velocity  $\int a_{0x}(t)dt$ :

$$\int_i a_{0x}(t)dt = \frac{r_x r_z}{r_y^2 + r_z^2} \left\{ -2r_z \int_i \left[ \frac{a_{1y}(t) - a_{0y}(t)}{2r_z} - \frac{a_{2x}(t)}{2r_y} \right] dt + 2r_y \int_i \left[ \frac{a_{3x}(t)}{2r_z} - \frac{a_{1z}(t) - a_{0z}(t)}{2r_x} \right] dt \right. \\ \left. + \frac{1}{\int_i \left[ \frac{a_{3x}(t) - a_{0x}(t)}{2r_x} - \frac{a_{1y}(t) - a_{0y}(t)}{2r_z} \right] dt} \left[ -2r_y \frac{a_{1y}(t) - a_{0y}(t)}{2r_z} + 2r_x \frac{a_{1z}(t) - a_{0z}(t)}{2r_x} - a_{2x}(t) + a_{3x}(t) \right] \right\} \quad (29)$$

The equation above allows for the calculation of the acceleration  $a_{0x}(t)$  when the other eight accelerations in the nine accelerometer array are known.

Similarly for the acceleration trace  $a_{0y}(t)$ , from the first equation of set 14:

$$a_{0y}(t) = -2r_z \left\{ \int_i \alpha_y(t) dt \int_i \alpha_x(t) dt - \frac{a_{2z}(t) - a_{0z}(t)}{2r_y} \right\} + a_{3y}(t) \\ = -2r_z \left\{ \int_i \left[ \frac{a_{3x}(t) - a_{0x}(t)}{2r_x} - \frac{a_{1z}(t) - a_{0z}(t)}{2r_x} \right] dt \int_i \left[ \frac{a_{1y}(t) - a_{0y}(t)}{2r_z} - \frac{a_{2x}(t) - a_{0x}(t)}{2r_y} \right] dt \right. \\ \left. - \frac{a_{2z}(t) - a_{0z}(t)}{2r_y} \right\} + a_{3y}(t) \quad (30a)$$

And by following the previous method, from the third equation of set 14:

$$a_{0y}(t) = -2r_x \left\{ \int_i \alpha_x(t) dt \int_i \alpha_y(t) dt - \frac{a_{2z}(t) - a_{0z}(t)}{2r_y} \right\} + a_{1y}(t) \\ = -2r_x \left\{ \int_i \left[ \frac{a_{2x}(t) - a_{0x}(t)}{2r_y} - \frac{a_{3y}(t) - a_{0y}(t)}{2r_z} \right] dt \int_i \left[ \frac{a_{3x}(t) - a_{0x}(t)}{2r_z} - \frac{a_{1z}(t) - a_{0z}(t)}{2r_x} \right] dt \right. \\ \left. - \frac{a_{2z}(t) - a_{0z}(t)}{2r_y} \right\} + a_{1y}(t) \quad (30b)$$

By subtracting 30b from 30a:

$$\int_i a_{0y}(t)dt = \frac{r_x r_z}{r_x^2 + r_z^2} \left\{ -2r_z \int_i \left[ \frac{a_{2x}(t) - a_{0x}(t)}{2r_y} - \frac{a_{3y}(t)}{2r_z} \right] dt + 2r_x \int_i \left[ \frac{a_{3x}(t)}{2r_z} - \frac{a_{1z}(t) - a_{0z}(t)}{2r_x} \right] dt \right. \\ \left. + \frac{1}{\int_i \left[ \frac{a_{3x}(t) - a_{0x}(t)}{2r_x} - \frac{a_{1y}(t) - a_{0y}(t)}{2r_z} \right] dt} \left[ 2r_y \frac{a_{2x}(t) - a_{0x}(t)}{2r_y} - 2r_z \frac{a_{3y}(t) - a_{0y}(t)}{2r_z} + a_{1y}(t) - a_{3y}(t) \right] \right\} \quad (31)$$

Again, for the acceleration trace  $a_{0z}(t)$ , from the first equation of set 14 we have:

$$a_{0z}(t) = -2r_y \left\{ \int_i \alpha_y(t) dt \int_i \alpha_x(t) dt - \frac{a_{3y}(t) - a_{0y}(t)}{2r_z} \right\} + a_{2z}(t) \\ = -2r_y \left\{ \int_i \left[ \frac{a_{3x}(t) - a_{0x}(t)}{2r_x} - \frac{a_{1z}(t) - a_{0z}(t)}{2r_x} \right] dt \int_i \left[ \frac{a_{1y}(t) - a_{0y}(t)}{2r_z} - \frac{a_{2x}(t) - a_{0x}(t)}{2r_y} \right] dt \right. \\ \left. - \frac{a_{3y}(t) - a_{0y}(t)}{2r_z} \right\} + a_{2z}(t) \quad (32a)$$

and from the second equation of set 14:

$$a_{0z}(t) = -2r_x \left\{ \int_i \alpha_x(t) dt \int_i \alpha_y(t) dt - \frac{a_{3y}(t) - a_{0y}(t)}{2r_z} \right\} + a_{1z}(t) \\ = -2r_x \left\{ \int_i \left[ \frac{a_{1y}(t) - a_{0y}(t)}{2r_z} - \frac{a_{2x}(t) - a_{0x}(t)}{2r_y} \right] dt \int_i \left[ \frac{a_{3x}(t) - a_{0x}(t)}{2r_z} - \frac{a_{1z}(t) - a_{0z}(t)}{2r_x} \right] dt \right. \\ \left. - \frac{a_{3y}(t) - a_{0y}(t)}{2r_z} \right\} + a_{1z}(t) \quad (32b)$$

By subtracting 32b from 32a:

$$\int_i a_{0z}(t)dt = \frac{r_x r_y}{r_x^2 + r_y^2} \left\{ -2r_z \int_i \left[ \frac{a_{3x}(t) - a_{0x}(t)}{2r_z} - \frac{a_{1z}(t)}{2r_x} \right] dt + 2r_y \int_i \left[ \frac{a_{2y}(t)}{2r_y} - \frac{a_{3y}(t) - a_{0y}(t)}{2r_z} \right] dt \right. \\ \left. + \frac{1}{\int_i \left[ \frac{a_{1y}(t) - a_{0y}(t)}{2r_z} - \frac{a_{2x}(t) - a_{0x}(t)}{2r_y} \right] dt} \left[ 2r_x \frac{a_{3x}(t) - a_{0x}(t)}{2r_z} - 2r_y \frac{a_{2y}(t) - a_{0y}(t)}{2r_z} + a_{1z}(t) - a_{3z}(t) \right] \right\} \quad (33)$$

The derived above equations 22 through 27, 29, 31, and 33 give the closed form solution for each acceleration trace in a NAAP configuration (Figure 1) as a function of the rest eight traces in the array, thus allowing for correction/calculation of any inaccurate/missing acceleration trace. An example in the Results section illustrates the use of these equations. It should be noted, however, that the closed form solutions above are given under the assumption of one inaccurate trace out of nine. If there are measuring errors in more than one trace then the optimization methodology similar to the one presented below should be utilized.

### Optimization Methodology for an In-plane Accelerometer Array Configuration

Consider a rigid body (Figure 4) with a set of translational accelerometers affixed to it at random locations with the known coordinates in a global coordinate system XYZ. For each point in Figure 4 equations similar to equations 5 can be written and solved for angular accelerations  $(\alpha_x, \alpha_y, \alpha_z)$ . These angular accelerations are then served as the design variables so that the cumulative error given in equation 34 is minimized at each time step between the measured translational accelerations and the

corresponding computed translational accelerations derived from equations 5.

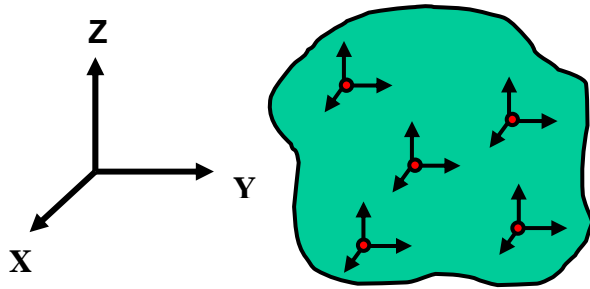


**Figure 4. Rigid body with accelerometers affixed to it at random locations.**

The objective function (error function) minimized at each time step is defined as:

$$\sqrt{\sum_{i=1}^n [(a_{ix}^m - a_{ix}^c)^2 + (a_{iy}^m - a_{iy}^c)^2 + (a_{iz}^m - a_{iz}^c)^2]} \quad (34)$$

where  $n$  is the number of points from which the acceleration data is obtained,  $m$  is the measured, and  $c$  is the computed data. This methodology allows for obtaining 3D angular accelerations that best satisfy all translational acceleration time histories at all given points.

## RESULTS

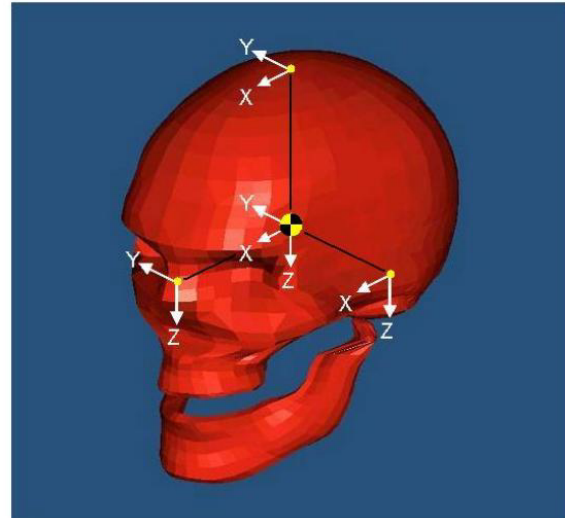
### Example of a Closed Form Solution

This example first takes a consistent set of nine accelerations from one of the NHTSA conducted NCAP tests, calculates angular accelerations using only Padgaonkar equations (12), then inputs these angular accelerations into a rigid body finite element model of a human skull (Figure 5) that calculates translational accelerations at the locations similar to those used in NAAP, and then compares the model output with the original measured translational accelerations.

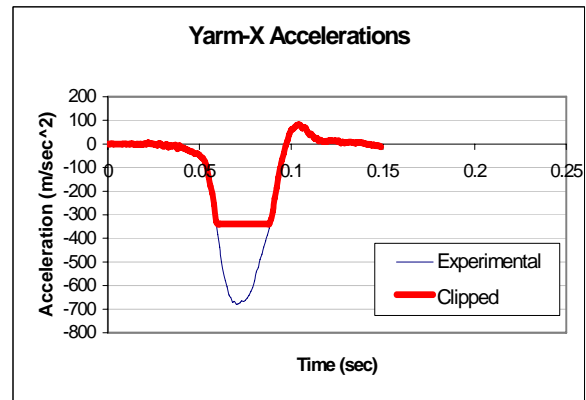
Next, one of the acceleration traces from the initially consistent set of nine accelerations was modified in the manner shown in Figure 6 in which the signal was clipped in half of its original amplitude. The purpose of this was to see the effect of this clipping procedure on the computed translational accelerations output from the model (Figure 7)

Figure 8 shows the results for the original and computed sets of accelerations confirming

consistency of the original set, Figure 9 shows the results of all nine traces after one of them was clipped.



**Figure 5. Rigid human finite element skull with accelerometer locations shown.**



**Figure 6. An original and clipped acceleration traces.**

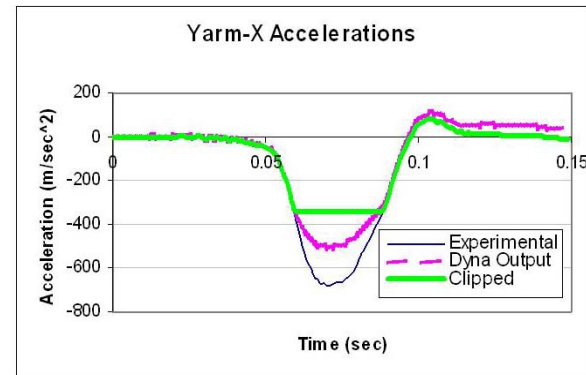


**Figure 7. An original (blue), clipped (green), and model output (magenta) acceleration traces.**

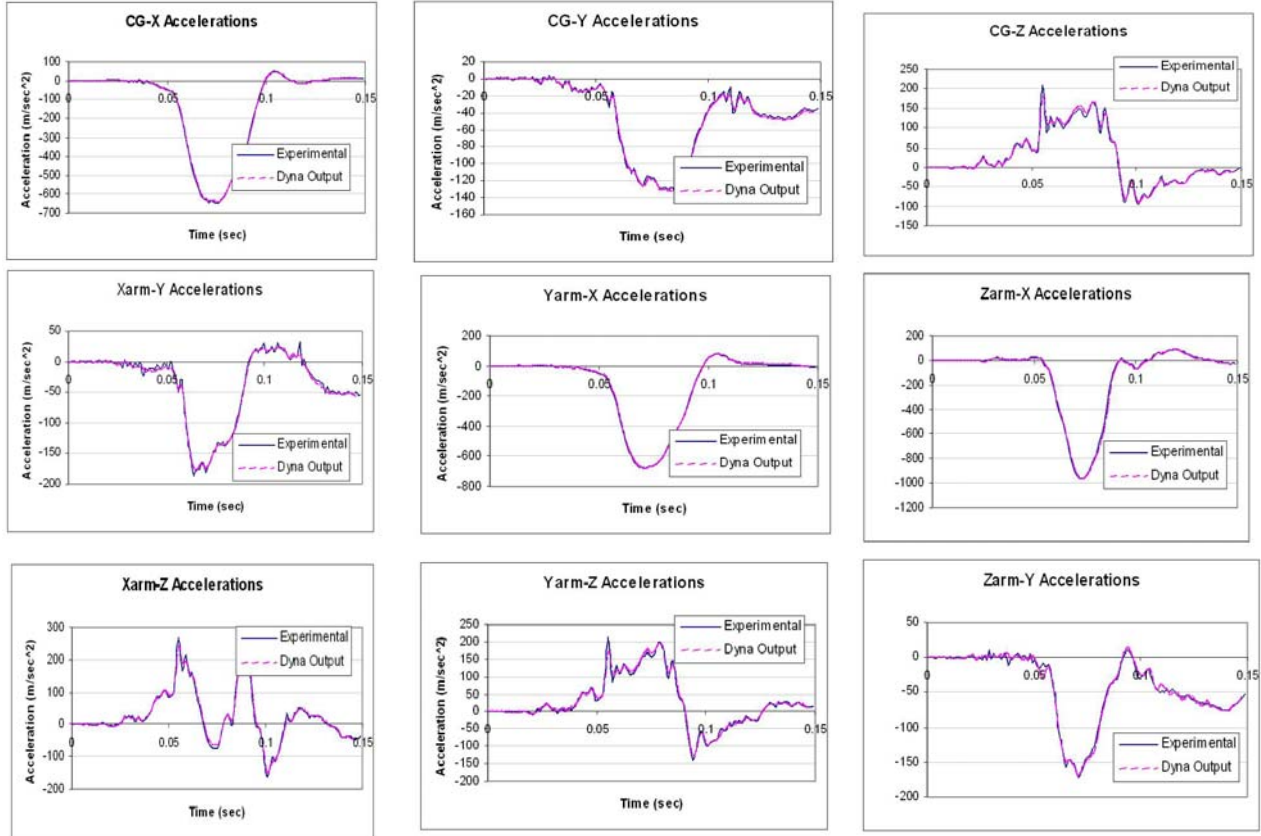


**Figure 8. Consistent set of nine accelerations.**

It is clear from Figure 9 that by clipping one of the original traces, then calculating angular accelerations using equations 12, and applying them to the finite element model, yields results that are inconsistent with the original set of translational accelerations. Interestingly, as illustrated in Figure 9, almost all of the original traces were affected by clipping only one of them. This illustrates the point that was made previously using equations 15 through 20.

The consistency/inconsistency of nine acceleration traces in NAAP can also be illustrated through the use of constraints equations (14). For a consistent set equations 14 will be satisfied, while opposite is true for an inconsistent set.

Equations 14, however, along with the derived above equations 22 through 27, 29, 31, and 33 can be used to identify and correct the erroneous trace. The procedure for this identification and correction is as follows:

1. Compute  $\alpha_x$ ,  $\alpha_y$ ,  $\alpha_z$  using original traces and Padgaonkar equations 12,
2. Compute products of angular velocities  $\omega_x\omega_y$ ,  $\omega_x\omega_z$ ,  $\omega_y\omega_z$  using rigid body constraint equations 14,

3. Compute each translational acceleration time history as a function of the remaining eight accelerations and radius vectors using equations 22 through 27, 29, 31, and 33,
4. Compare computed and original eight translational accelerations (excluding the one under consideration) and find their cumulative error using equation similar to 34,
5. When the cumulative error is very small, the erroneous trace is found and it should be substituted with its computed equivalent.

When the described above procedure was applied to the set of nine acceleration traces with one of them clipped, the clipped trace was identified and substituted with its computed equivalent giving results similar to the one shown in Figure 8 with all the traces overlapping each other.

### Optimization Methodology Example

Consider a small triangular plate with accelerometers mounted in the manner shown in Figure 10. The small size of the plate is chosen such that it fits into a mouthpiece of a boxer, football or hockey player.

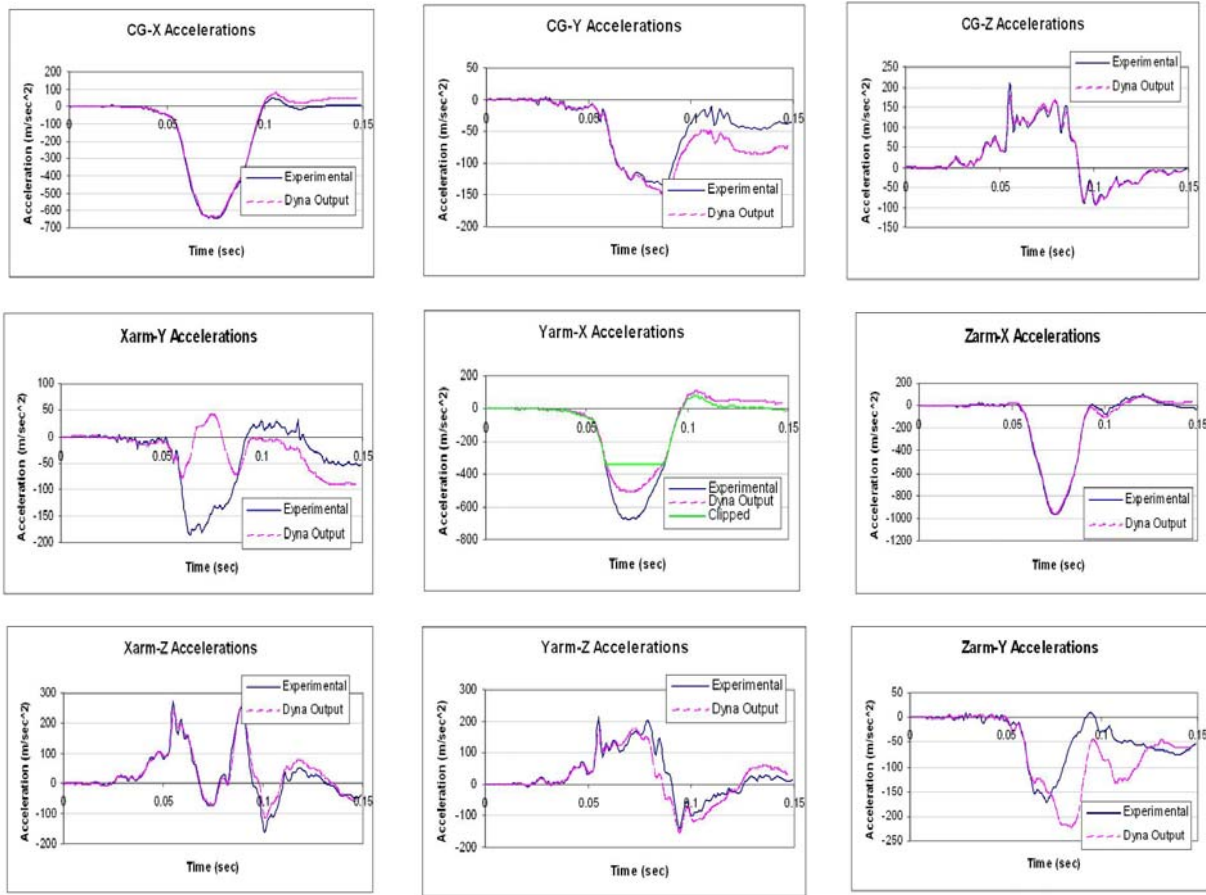


Figure 9. Inconsistent set of nine accelerations (magenta) as compared with the original consistent set (blue).

Using the general equations 5, translational accelerations shown in Figure 10 can be expressed as:

$$\begin{bmatrix} a_{1x} \\ a_{1y} \\ a_{1z} \end{bmatrix} = \begin{bmatrix} a_{2x} \\ a_{2y} \\ a_{2z} \end{bmatrix} + \begin{bmatrix} 0 \\ \alpha_z r_x \\ -\alpha_y r_x \end{bmatrix} + \begin{bmatrix} -r_x(\omega_y^2 + \omega_z^2) \\ \omega_y(\omega_x r_x) \\ \omega_z(\omega_x r_x) \end{bmatrix} \quad (35)$$

$$\begin{bmatrix} a_{2x} \\ a_{2y} \\ a_{2z} \end{bmatrix} = \begin{bmatrix} a_{1x} \\ a_{1y} \\ a_{1z} \end{bmatrix} - \begin{bmatrix} 0 \\ \alpha_z r_x \\ -\alpha_y r_x \end{bmatrix} - \begin{bmatrix} -r_x(\omega_y^2 + \omega_z^2) \\ \omega_y(\omega_x r_x) \\ \omega_z(\omega_x r_x) \end{bmatrix} \quad (36)$$

$$\begin{bmatrix} a_{3x} \\ a_{3y} \\ a_{3z} \end{bmatrix} = \begin{bmatrix} a_{1x} \\ a_{1y} \\ a_{1z} \end{bmatrix} + \begin{bmatrix} -\alpha_z r_y \\ \alpha_x \frac{1}{2} r_x \\ \alpha_x r_y - \alpha_y \frac{1}{2} r_x \end{bmatrix} + \begin{bmatrix} \omega_x(\omega_y r_y) - \frac{1}{2} r_x(\omega_y^2 + \omega_z^2) \\ \omega_y(\omega_x \frac{1}{2} r_x) - r_y(\omega_z^2 + \omega_x^2) \\ \omega_z(\omega_x \frac{1}{2} r_x + \omega_y r_y) \end{bmatrix} \quad (37)$$

where  $\alpha_x, \alpha_y, \alpha_z$  are angular accelerations of the plate,  $\omega_x, \omega_y, \omega_z$  are angular velocities, and  $r_x, r_y, r_z$  are distances between points 1, 2, and 3 in the directions X, Y, and Z respectively.

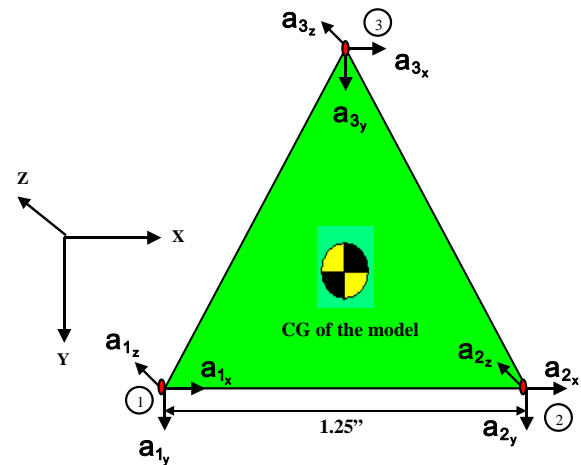
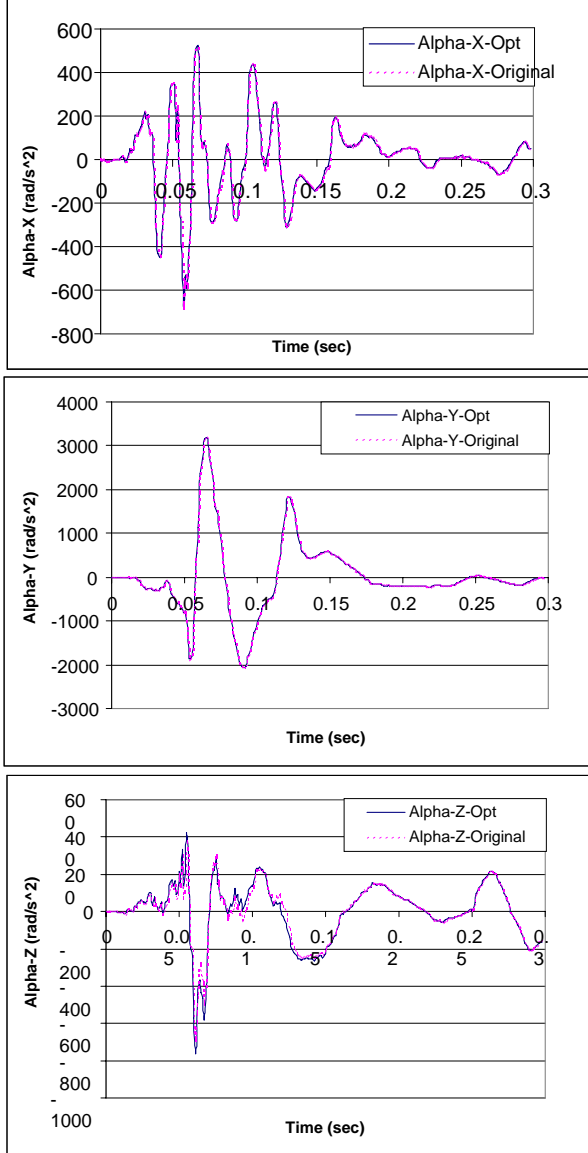


Figure 10. Small triangular plate setup with nine accelerometers fixed at points 1, 2, and 3.

Using numerical finite element model of the rigid triangular plate an arbitrary 3D motion was applied to

generate the nine consistent traces. Figure 11 shows comparison of the angular accelerations from the finite element model with those obtained using optimization (equations 35 – 37, and 34 as an objective function).



**Figure 11. Original versus optimized angular accelerations.**

Assume now that there is a 3% cross-axis sensitivity error for each tri-axial accelerometer located at points 1, 2, and 3 in Figure 10. This error can be expressed as:

$$\begin{aligned}
 a_{ix} &= a_{ix} + 0.03a_{iy} + 0.03a_{iz} \\
 a_{iy} &= a_{iy} + 0.03a_{ix} + 0.03a_{iz} \\
 a_{iz} &= a_{iz} + 0.03a_{ix} + 0.03a_{iy}
 \end{aligned}
 \quad i = 1 \text{ to } 3. \quad (38)$$

When the new (erroneous) accelerations (38) are used in place of the old traces obtained from finite element simulation and the optimization procedure, described above, applied to this new set of accelerations, the resulting angular accelerations are identical to those shown in Figure 11.

This procedure demonstrates the applicability of the optimization methodology to recover proper set of acceleration traces when some of the channels are contaminated with random errors. The closed form solution for this hypothetical situation is not currently available.

## DISCUSSION

This paper demonstrates some of the limitations in the use of NAAP when only Padgaonkar equations (12) are considered. In particular, if one or more of the accelerometers in the array are not measured properly, the resulting kinematics of a rigid body is substantially affected because these errors are present in the computed angular accelerations. To correct for these possible errors, two methods were derived in this paper and their use was demonstrated.

The first method – the closed form solution - uses additional constraint equations (14) to express each accelerometer in the array as a function of the other eight. The computed and original translational accelerations can then be compared, erroneous acceleration identified, and replaced. This method is limited to the cases when one of the acceleration traces is incorrect. It was also demonstrated that nine accelerations in the NAAP are not independent of each other, but rather bound by the rigid body constraints. This is somewhat intuitive because a rigid body has six degrees of freedom and any additional measure beyond six must be governed by an additional constraint. In the case of NAAP, three additional accelerations are governed by three additional constraints – equations 14.

The second method – the optimization method – uses angular accelerations as design variables for the objective function set to minimize the differences/errors between the measured and computed translational accelerations. This method, although not as elegant as the first one, can be used when multiple channels of accelerations in NAAP or any other configuration are not measured properly.

Both methods can be used by the biomechanical laboratories to analyze and gain confidence in the measures of angular kinematics of human or dummy heads.

## CONCLUSIONS

The paper presents two methodologies to analyze angular kinematics of a rigid body when an array of translational accelerometers is used as the motion sensing device. It was demonstrated that:

- Nine accelerometer measures in NAAP are not independent, but rather constrained,
- The constraint equations can be derived and used to identify and correct an erroneous acceleration trace using a closed form solution method,
- The closed form solution method is limited to one erroneous accelerometer trace in the array,
- Optimization methodology can be utilized to correct errors in multiple channels of translational accelerometers.

## REFERENCES

- [1] Hardy, W.N., Foster, C., Mason, M., Yang, K., King, A., Tashman, S., 2001, "Investigation of head injury mechanisms using neutral density technology and high-speed biplanar X-ray". *Stapp Car Crash Journal* 45. pp. 337-368.
- [1] Hardy, W.N., Mason, M., Foster, C.D., Shah, C.S., Kopacz, J.M., Yang, K.H., King, A.I., 2007, "A study of the Response of the Human Cadaver Head to Impact". *Stapp Car Crash Journal* 51, pp. 17-80.
- [3] Takhounts, E.G., Eppinger, R.H., Campbell, J.Q., Tannous, R.E., Power, E.D., Shook, L.S., 2003, "On the Development of the SIMon Finite Element Head Model". *Stapp Car Crash Journal* 47, pp. 107-133.
- [4] Takhounts, E.G., Hasija, V., Ridella, S.A., Tannous, R.E., Campbell, J.Q., Malone, D., Danelson, K., Stitzel, J., Rowson, S., Duma, S., 2008, "Investigation of Traumatic Brain Injuries Using the Next Generation of Simulated Injury Monitor (SIMon) Finite Element Head Model." *Stapp Car Journal* 52, pp 1 – 32.
- [5] Pagaonkar, A.J., Krieger, K.W., and King, A.I., 1975. "Measurement of angular acceleration of a rigid body using linear accelerometers". *Journal of Applied Mechanics*, pp. 552-556.